

# Multi-direction digital moving mask method for fabricating continuous microstructures

ZHIMIN ZHANG<sup>1,2</sup>, YIQING GAO<sup>2</sup>, NINGNING LUO<sup>2</sup>, KEJUN ZHONG<sup>1,2</sup>, ZHIHUI LIU<sup>3</sup>

<sup>1</sup>College of Automation Engineering, Nanjing University of Aeronautics and Astronautics, Nanjing 210016, China

<sup>2</sup>Key Laboratory of Nondestructive Test (Chinese Ministry of Education), Nanchang Hangkong University, Nanchang 330063, China

<sup>3</sup>Optoelectronics Division, Jiangxi Lianchuang Optoelectronic Technology Co., Ltd., Nanchang, 330096, China

\*Corresponding author: ningningluo2002@126.com

The multi-direction digital moving mask method, employing the superposition of the exposure along various moving directions, is developed for fabricating continuous microstructures. The mask pattern corresponding to each moving direction is determined by projecting the target dose profile in the corresponding moving direction. All the mask patterns are dynamically exposed on the same substrate layer by layer so as to form a 3D profile of the exposure dose. The selection criterion of a quantization number and moving-direction number is discussed. For verification of the multi-direction moving method, experiments are performed to fabricate a square pyramid array and square-based microlens array by moving along two orthogonal directions, and round-based microlens array by moving along six directions.

Keywords: multi-direction digital moving mask, superposition, quantization.

## 1. Introduction

During the past decade, continuous microstructures generated by lithographic techniques are increasingly applied in the areas of microoptics, microelectronics, microelectromechanical systems (MEMS) and integrated circuits [1–6]. However, largely owing to the dramatic increase in mask cost and cycle time, there is a strong incentive to develop a high efficiency maskless lithography. As an alternative technique, the optical maskless lithography (OML) based on digital micromirror devices (DMD) is growing rapidly due to the distinct advantages of the flexibility of digital masks and the parallelism of projection photolithography [7–10]. Various methods including the grayscale [11], the moving mask [12] and the virtual layering [13–15], have been developed to extend the application of DMD-based OML.

We have previously reported the digital moving mask method to form line-symmetry microstructures such as micro-cylindrical lens and blazed grating arrays [12], in which the digital mask was controlled to only move in a single direction. In comparison with DMD-based gray-scale lithography, the digital moving mask patterns are binary. Therefore, the digital moving mask method relieves from the burdens associated with the nonlinear modulation characteristics of DMD. However, the exposure dose distribution in the moving direction cannot be changed when the mask is given. Thus, the types of fabricated microstructures are limited due to the single moving direction. Microstructures such as microlens cannot be manufactured with the single-direction method. Besides, in the single-direction method, the mask is designed according to the target profile. There is no uniform rule for determining the mask pattern.

In this paper, the multi-direction digital moving mask method is proposed to satisfy the requirements in fabricating more complex microstructures such as rotation-symmetry relief, which cannot be fabricated by the single-direction method. Although more moving directions are involved in the multi-direction method, it need not repeat calibration because the exposure position is precisely determined by DMD pixel. The experimental system and principle of the method are described. To fabricate microstructures precisely, we also discuss the selection criterion of the important parameters in the mask design, including quantization number and the moving-direction number. Experimental fabrication of microlens and square pyramid structures is discussed for evaluating the proposed method.

## 2. Principle

### 2.1. Digital moving mask system

A schematic of the digital moving mask system is shown in Fig. 1. The system comprises five major components: uniform illumination system, DMD, projection lens, photoresist, and motorized stage.

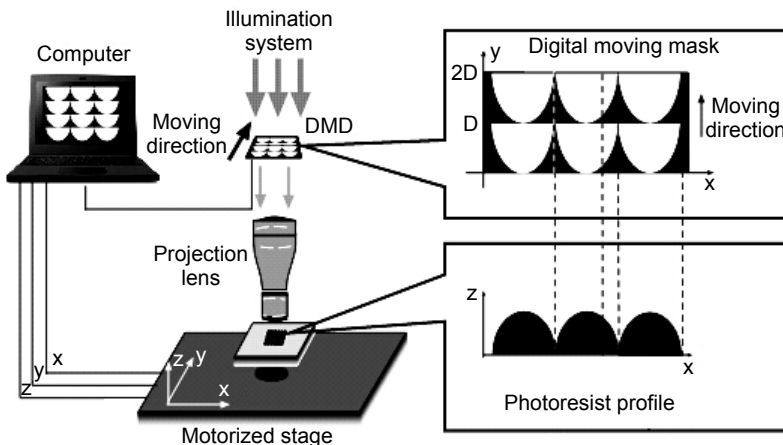


Fig. 1. Schematic of the digital moving mask system.

motorized stage, and computer. A 200 W mercury short arc lamp (OSRAM Co.) is used as a light source. The illumination light (365 nm) is homogenized by a fly eye before striking the DMD. The Texas Instruments DMD consists of  $1024 \times 768$  micromirrors having a pitch size of  $13.68 \mu\text{m}$ . The  $0.071 \times$  projection lens with numerical aperture of 0.3 is vertically installed to reduce the DMD image. The DMD can project the pattern covering an area of approximately  $1.01 \text{ mm} \times 0.75 \text{ mm}$ , including  $1024 \times 768$  pixels, each of which is  $0.977 \mu\text{m}$  in size. The motorized stage includes  $XY$  stages and  $Z$  stage.  $XY$  stages cover a total range of  $3 \times 3 \text{ cm}^2$  with accuracy of  $\pm 0.65 \mu\text{m}$ .  $Z$  stage covers a range of 2 mm with accuracy of  $\pm 1 \mu\text{m}$ . A computer is used to control the motorized stage and DMD.

During exposure, uniform UV light is irradiated onto micromirrors in DMD and then is selectively reflected toward the projection lens. The reflected pattern plays the role of a virtual mask. When the mask is stationary, the mask pattern can be copied to the photoresist after development. While the mask is controlled to move along one or more directions, the exposure dose on the photoresist can be modulated continuously by the shape of the mask pattern.

## 2.2. Principle of multi-direction digital moving mask for fabricating microstructure

For fabricating line-symmetry microstructures, only one moving direction is needed. To achieve more complex continuous relief, we propose the multi-direction digital moving mask method schematically depicted in Fig. 2.

First, we must determine the moving-direction number according to the target dose profile as shown in Fig. 2a. Next, the moving directions are uniformly selected within a 180-degree range according to the symmetry of projection. Then, projecting the 3D dose profile in the corresponding moving direction, 2D projection corresponding to each moving direction can be obtained. After quantization in a certain region,

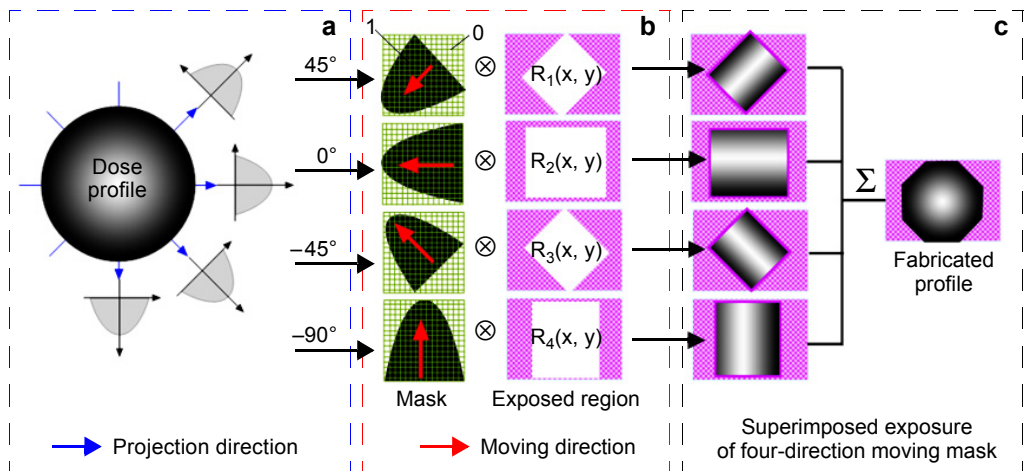


Fig. 2. Schematic of the multi-direction digital moving mask method (see text for explanation).

the 2D binary mask pattern can be obtained as shown in Fig. 2b. The selection criterion of a quantization number will be discussed in detail in the next section. During exposure each mask pattern is controlled to circularly move in the quantization region along the corresponding direction. Finally, the mask patterns corresponding to various moving directions are dynamically exposed on the same substrate layer by layer so as to form a 3D profile of the exposure dose in Fig. 2c. The above superimposition procedure is relieved from the burdens associated with alignment because the initial position and the end point of the mask can be precisely controlled by a computer.

The exposure dose in each moving direction is modulated by the corresponding mask and can be regarded as a circular convolution between the mask  $M_j(x, y)$  and the corresponding exposed region  $R_j(x, y)$ . So the exposure dose distribution  $E_j(x, y)$  can be written as

$$E_j(x, y) = cM_j(x, y) \otimes R_j(x, y) \quad (1)$$

where  $M_j(x, y) = \begin{cases} 0, & (x, y) \notin R_j(x, y) \\ 1, & (x, y) \in R_j(x, y) \end{cases}$ , and  $c$  is the parameter related to the exposure process. So the exposure dose distribution on the photoresist corresponding to the target microstructure can be approached from the superposition of the exposure along each moving direction

$$E(x, y) = \sum_{j=1}^N E_j(x, y) = c \sum_{j=1}^N M_j(x, y) \otimes R_j(x, y) \quad (2)$$

where  $N$  is the number of moving directions.

### 2.3. Selection criterion of a quantization number

In the design of a mask pattern, the quantization number  $L$  is an important parameter, which will directly affect the distribution of an exposure dose. In this section we give a criterion for determining it reasonably basing on the mean error between the target dose profile and the superposition dose profile achieved by the moving mask method. Here, suppose a square-based microlens is the target microstructure, then we can determine by experience that two exposure processes, perpendicular to each other, are needed. The exposure dose distribution corresponding to the target microlens can be approached from the superposition of the exposure along two orthogonal directions.

To obtain the mean error between the target dose profile and the superposition dose profile, the exposure simulation is performed by changing the quantization number  $L$  from 1 to 50 and  $L$  should be an integer. In simulation, the moving speed is 12  $\mu\text{m/s}$ . From the error in Fig. 3, we know that the mean error gradually decreases and tends to become stable with the increase in the quantization number. Theoretically speaking,  $L$  should be large enough to fulfill the precision of the mask pattern. If  $L \geq 10$ , the mean error can be kept under 5%. Suppose that when the mean error is kept under 2%,

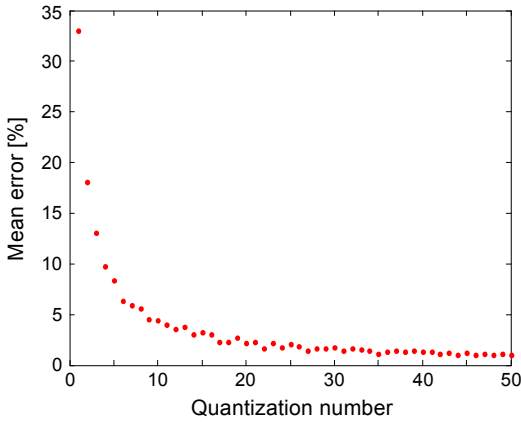


Fig. 3. Mean error between the target dose profile and the superposition dose profile obtained by changing the quantization number.

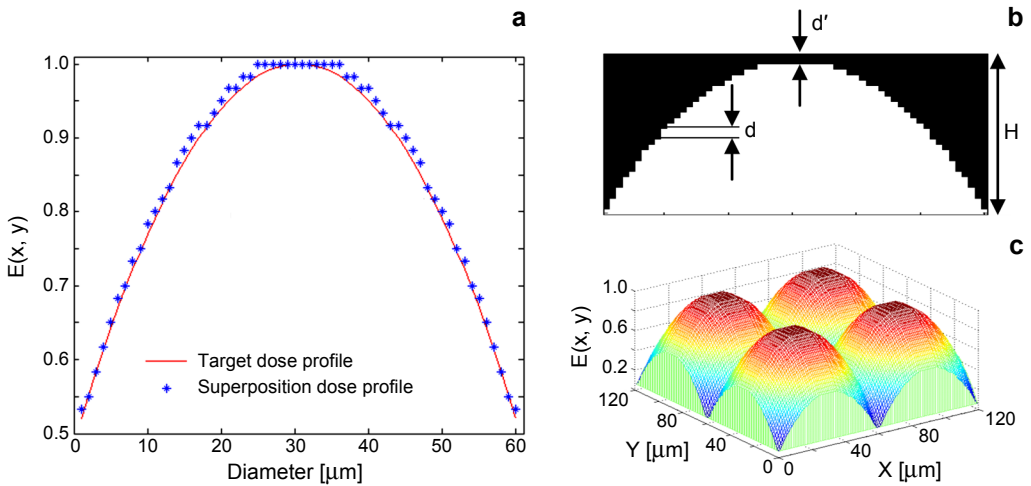


Fig. 4. Simulation results of square-based microlens. Cross-section of the target dose profile and the superposition dose profile (a), moving mask pattern (b), and superposition dose profile of a microlens array (c).

the precision of the mask pattern can be ensured, then  $L \geq 26$  should be taken. In our following cases, we take the quantization number  $L = 30$ , and the corresponding mean error is 1.73%. When  $L = 30$ , the target dose profile and the superposition dose profile are simulated as shown in Fig. 4a, where the solid line shows the target dose profile, and the asterisk shows the superposition dose profile. From Fig. 4a, we can know that the top of the superposition dose profile becomes flat compared with the target dose profile denoted by the solid line. Part of the superposition profile arrays are shown in Fig. 4c, from which we can also see that the profile top approximates to a square.

The quantization mask is shown in Fig. 4b. Suppose the height of the quantization region is  $H$ , we can obtain the height of each step  $d = H/L$ .

#### 2.4. Determination of a moving-direction number

In the method of a multi-direction digital moving mask, the moving-direction number should be determined first. Theoretically speaking, with the moving-direction number  $N$ , we can obtain a polygon profile with  $2N$  edges. When  $N$  becomes larger, a polygon can approximate to a circle, which fulfills the requirement of a round-based microlens. Although the precision and roughness of the microlens profile can be the best when  $N$  becomes large enough, the whole exposure process will be more time-consuming. The smallest  $N$ , which can ensure the precision and roughness of microlens profile, can be determined based on the mean error between the target dose profile and the superposition dose profile achieved through multi-direction moving. The exposure doses are simulated by varying the integer value of  $N$  from 1 to 20. In simulation, the moving speed is  $12 \mu\text{m/s}$  and the quantization number  $L = 30$ . The error curve between the target dose profile and the superposition dose profile is shown in Fig. 5, from which we can see that when  $N \leq 4$ , the mean error decreases markedly with the increase in  $N$ . Figure 5 also shows that the mean error is almost unchanged with  $N$  increasing above 6. In the following experiment for round-based microlens, the smallest moving-direction number we can take is  $N = 6$ , which corresponds to the mean error of 1.41%.

### 3. Experiments and discussion

To evaluate the validity of the multi-direction digital moving mask method, the lithography for a square pyramid and microlens has been performed. Here the square pyramid and the square-based microlens are fabricated by moving along two orthogonal direc-

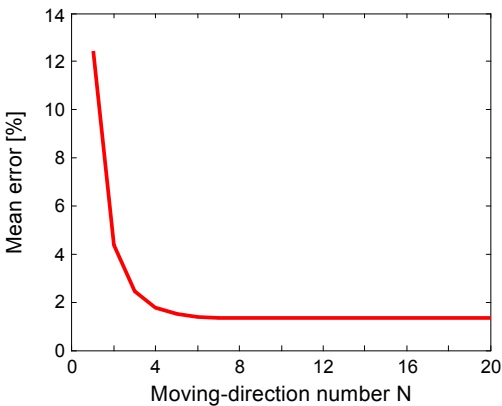


Fig. 5. Error curve between the target dose profile and the superposition dose profile obtained by changing a moving-direction number.

tions, while the round-based microlens by six directions. In the experiments, we use a positive photoresist of GP-28, which is spin-coated on a glass substrate. After the spin coating at 1000 rpm and a soft baking for 30 min at 100°C, about a 4 μm thick photoresist layer is obtained. The multi-direction mask patterns are then exposed on the pho-

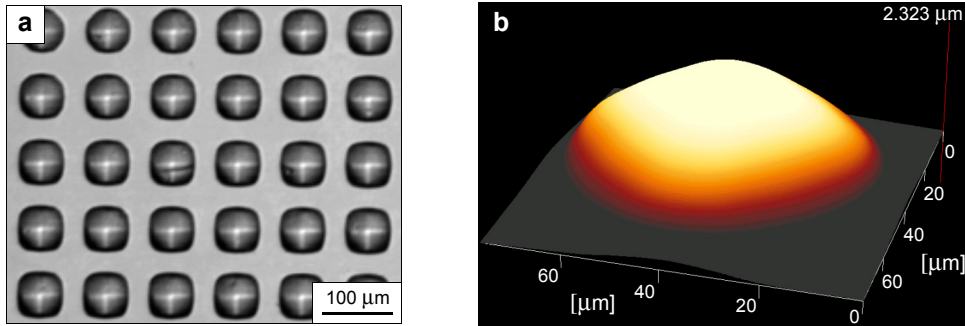


Fig. 6. Fabricated photoresist square pyramid. Optical micrograph (a) and profile measured by MicroXAM-100 optical profilometer (b).

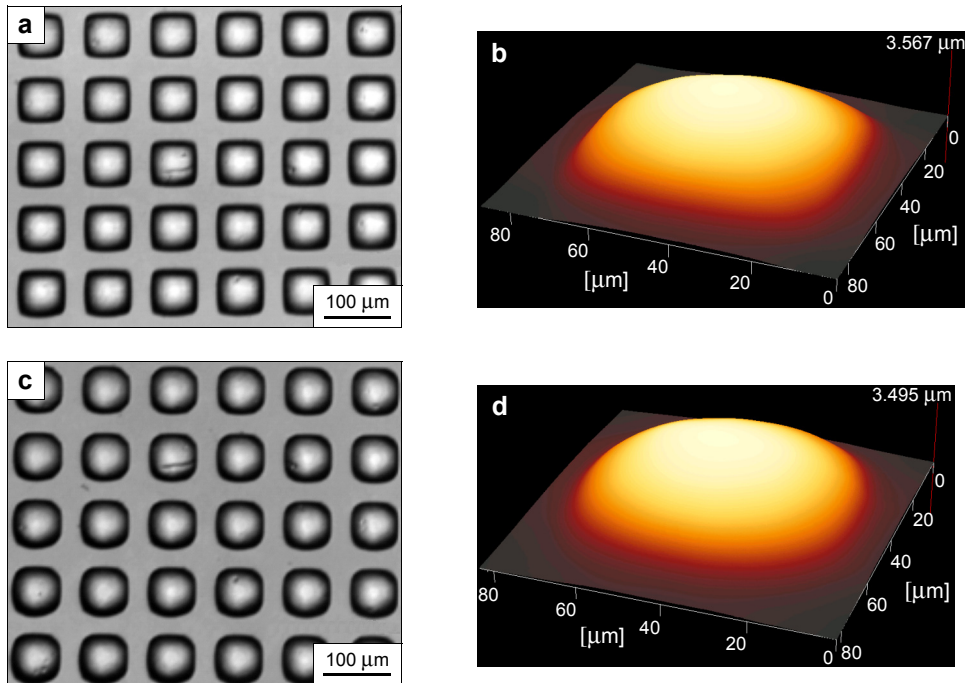


Fig. 7. Fabricated photoresist microlens array. Optical micrograph of a square-based microlens array (a). Profile of a single microlens with a square base (b). Optical micrograph of a round-based microlens array (c). Profile of a single microlens with a round base (d).

toresist-coated glass substrate. The total exposure time is 20 s for two directions, and 21 s for six directions. After development in NaOH developer for about 10 s, the profiles of a square pyramid and microlens are obtained.

Figure 6 shows the fabricated result of a square pyramid. The optical micrograph of the fabricated photoresist pattern of the arrayed square pyramid is shown in Fig. 6a. The 3D profile of a square pyramid measured by MicroXAM-100 optical profilometer (KLA-Tencor Inc.) is shown in Fig. 6b, with an edge length of 62.2  $\mu\text{m}$  and height of 2.3  $\mu\text{m}$ . Figure 7 shows the fabricated results of a microlens. Optical micrograph of the fabricated photoresist pattern of a square-based microlens array is shown in Fig. 7a. The 3D profile of a single microlens in Fig. 7a is measured, as shown in Fig. 7b, with the diameter of 63.4  $\mu\text{m}$  and the height of 3.39  $\mu\text{m}$ ; Fig. 7c is the optical micrograph of the photoresist microlens with a round base; Fig. 7d shows the 3D profile of a single microlens in Fig. 7c, with the measured diameter of 63.1  $\mu\text{m}$  and the measured height of 3.45  $\mu\text{m}$ . Figures 6 and 7 reveal that the uniform patterns with smooth surface are achieved. The profile error is analyzed by fitting the target profile to the measured data as shown in Figs. 8a and 8b, respectively, for square-based and round-based microlens, where the solid curve shows the target profile and the diamonds show the measured one. The relative errors between the measured profile and the target profile are shown in Fig. 8c and 8d, from which we can see that the maximum relative errors are 7.16% and 6.22%, respectively for square-based and round-based microlens.

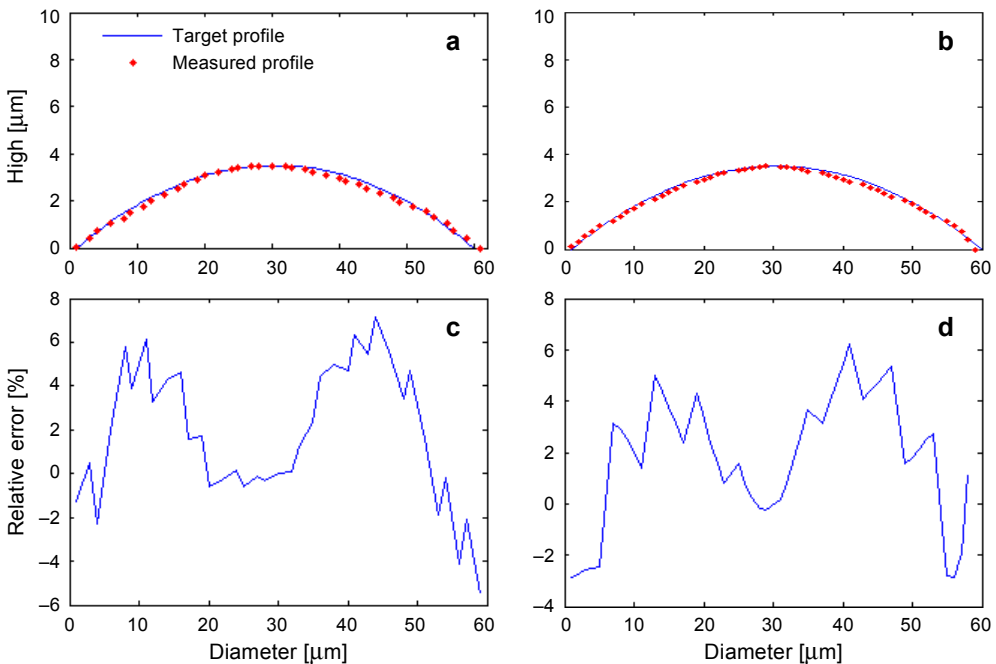


Fig. 8. Profile error. Curves of the target profile and the measured profile of the square-based (a) and round-based (b) microlens. Relative error between the target profile and the measured profile of the square-based (c) and round-based (d) microlens.

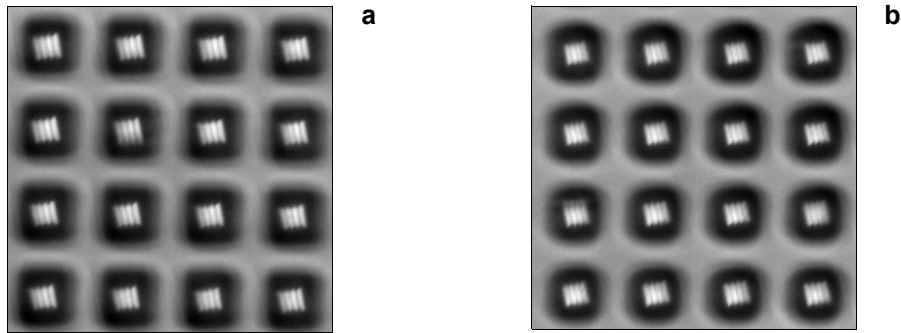


Fig. 9. Image arrays of filament generated by a microlens array under white light illumination by a square-based (a) and round-based (b) microlens array.

The focal length of each microlens is  $181\ \mu\text{m}$  for square-based microlens, and  $183\ \mu\text{m}$  for round-based microlens, which is measured using a set of microscopy imaging system at  $532\ \text{nm}$ . Arrayed microlens can generate good images under white light illumination when used in reflection case, which is proved by Fig. 9. It shows the image arrays of a filament generated by microlens arrays. Figure 9 can be easily taken by using MicroXAM-100 optical profilometer and the use of only one beam illumination, the interference light beam is taken off.

#### 4. Conclusions

In this study, the multi-direction digital moving mask method has been developed for fabricating complex continuous microstructures, which makes the working range for the digital moving mask method greatly expanded. The potential of the proposed method for fabricating microstructures is confirmed through theoretical and experimental studies. As examples, the photoresist profile fabrication of microlens arrays by two or even six directions and a square pyramid by two directions has been demonstrated. The proposed method has two major advantages. One is to satisfy the requirements in fabricating various types of continuous microstructures, especially for the microstructures which cannot be realized by the single-direction method. The other is to avoid the nonlinear modulation of DMD by using a binary mask pattern compared with the digital gray lithography.

*Acknowledgments* – The work is supported by the National Natural Science Foundation of China (61464008 and 61261026) and the Natural Science Foundation of Jiangxi Province (20142BAB217003).

#### References

- [1] REN YANG, SOPER S.A., WANJUN WANG, *Microfabrication of pre-aligned fiber bundle couplers using ultraviolet lithography of SU-8*, *Sensors and Actuators A: Physical* **127**(1), 2006, pp. 123–130.
- [2] CAIJUN KE, XINJIAN YI, ZHIMOU XU, JIANJUN LAI, *Monolithic integration technology between microlens arrays and infrared charge coupled devices*, *Optics and Laser Technology* **37**(3), 2005, pp. 239–243.

- [3] EITEL S., FANCEY S.J., GAUGGEL H.-P., GULDEN K.H., BACHTOLD W., TAGHIZADEH M.R., *Highly uniform vertical-cavity surface-emitting lasers integrated with microlens arrays*, IEEE Photonics Technology Letters **12**(5), 2000, pp. 459–461.
- [4] CHANGQING YI, CHEUK-WING LI, SHENGLIN JI, MENG SU YANG, *Microfluidics technology for manipulation and analysis of biological cells*, Analytica Chimica Acta **560**(1–2), 2006, pp. 1–23.
- [5] ZHANG X., JIANG X.N., SUN C., *Micro-stereolithography of polymeric and ceramic microstructures*, Sensors and Actuators A: Physical **77**(2), 1999, pp. 149–156.
- [6] CHENG SUN, XIANG ZHANG, *The influences of the material properties on ceramic micro-stereolithography*, Sensors and Actuators A: Physical **101**(3), 2002, pp. 364–370.
- [7] YIQING GAO, TINGZHENG SHEN, JINSONG CHEN, NINGNING LUO, XINMIN QI, QI JIN, *Research on high-quality projecting reduction lithography system based on digital mask technique*, Optik – International Journal for Light and Electron Optics **116**(7), 2005, pp. 303–310.
- [8] YI LU, SHAOCHEN CHEN, *Direct write of microlens array using digital projection photopolymerization*, Applied Physics Letters **92**(4), 2008, article 041109.
- [9] KESSELS M.V., NASSOUR C., GROSSO P., HEGGARTY K., *Direct write of optical diffractive elements and planar waveguides with a digital micromirror device based UV photoplotter*, Optics Communications **283**(15), 2010, pp. 3089–3094.
- [10] XIAOWEI GUO, JINGLEI DU, YONGKANG GUO, CHUNLEI DU, ZHENG CUI, JUN YAO, *Simulation of DOE fabrication using DMD-based gray-tone lithography*, Microelectronic Engineering **83**(4–9), 2006, pp. 1012–1016.
- [11] TOTSU K., FUJISHIRO K., TANAKA S., ESASHI M., *Fabrication of three-dimensional microstructure using maskless gray-scale lithography*, Sensors and Actuators A: Physical **130–131**, 2006, pp. 387–392.
- [12] YIQING GAO, NINGNING LUO, TINGZHENG CHEN, MIN CHEN, *Research on digital mask fabrication technique of micro-optical element*, Journal of Modern Optics **56**(4), 2009, pp. 453–462.
- [13] MANSEUNG SEO, HAERYUNG KIM, *Influence of dynamic sub-pixelation on exposure intensity distribution under diffraction effects in spatial light modulation based lithography*, Microelectronic Engineering **98**, 2012, pp. 125–129.
- [14] MANSEUNG SEO, HAERYUNG KIM, *Spatial light modulation based 3D lithography with single scan virtual layering*, Microelectronic Engineering **88**(8), 2011, pp. 2117–2120.
- [15] JUN-GYU HUR, *Maskless fabrication of three-dimensional microstructures with high isotropic resolution: practical and theoretical considerations*, Applied Optics **50**(16), 2011, pp. 2383–2390.

*Received November 10, 2014  
in revised form December 16, 2014*